The Journal of Engineering Geology, Vol.4, No.3, December., 1994, pp.283-295.

Nonstationary Dual-Porosity Fractal Model of Groundwater Flow in Fractured Aquifers with or without Fracture Skin

균열 스킨을 포함하거나 포함하지 않는 균열 대수층내 지하수 유동에 관한 비정상류의 이중공극 프락탈 모델

함 세 영(Hamm, Se-Yeong) 한국자원연구소
Bidaux, Pasal University of Montpellier II

Abstract/요약

A new nonstationary dual-porosity fractal model is presented which simulates a nonsteady state block-to-fissure flow with or without fracture skin between the block and the fissure in a fractal aquifer. The model includes wellbore storage and well loss effects on the production well. Type curves for different flow dimensions with different values of hydraulic parameters are created.

The application of the model to experimental data in fractured aquifer is described.

새로운 비정상류 이중공극 프락탈 모델이 소개되었다. 이 모델은 프락탈대수층내에서 블록으로부터 균열로 향하는 비정상류 및 블록과 균열간의 스킨을 모식화한 것이다. 이 모델은 또한 양수정의 우물저장과 우물손실효과를 포함한다. 이 모델에 의해서 여러가지 흐름의 차원과 여러가지 값의 수리상수에 대한 표준곡선들이 만들어졌다.

이 모델은 균열 대수층의 야외 자료에 적용되었다.

INTRODUCTION

Several dual-porosity models for simulating fissured rock has been described by a certain number of authors(Barenblatt et al., 1960 ; Warren and Root, 1963 ;

Kazemi, 1969 ; Streltsova, 1976 ; Boulton and Streltsova, 1977 ; Moench, 1984). The dual-porosity model is classified into two categories : one assumes steady state flux from a block to a fissure(Barenblatt et al., 1960 ; Warren and Root, 1963) and the other assumes nonsteady state flow from a block to a fissure(Kazemi, 1969 ; Boulton and Streltsova, 1977).

All the models mentioned above can only treat integral flow dimensions while the groundwater flow in fractured rocks is controlled by the fracture network which often shows a fractal geometry(Allègre, 1982 ; Thomas, 1987 ; Velde et al., 1991). Ground water flow analysis by the fractal theory has been introduced to hydrodynamics by Barker (1988) and by Chang and Yortsos(1988). Thus, we can consider fractal models which account for groundwater flow in fractal aquifers composed of fractal network of fractures. Hamm and Bidaux(1994a) proposed the fractal model of flow with leakage from semipermeable layer. The stationary double-porosity fractal model of groundwater flow was proposed by Hamm and Bidaux(1944b). One of the important points in the fractal models is the non-integer flow dimension.

In this paper, the authors derived a nonstationary dual-porosity fractal model with or without skin fracture(Fig. 1). It also takes into consideration the wellbore storage and skin effects at the pumped well, and can be easily utilized for the multi-well and multi-rate pumping system composed of several production and observation wells.

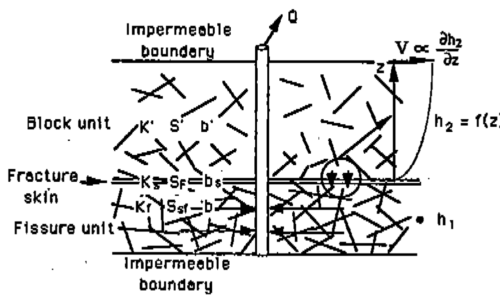

Fig. 1 Nonstationary dual-porosity fractal model.

THEORY

The nonstationary dual-porosity theory comprises non-steady block-to-fissure flow. Non-stationary flux between the block and the fracture induces a difficulty due to the flow of interior of blocks. So, it is required to know the form and the size of the blocks. In spite of this difficulty, we consider that both the fissures and the blocks overlap and they are related to each other as a total volume. Furthermore, the parameters K_f (hydraulic conductivity of the fissure), S_{sf} (specific storage of the fissure) and S_s' (specific storage of the matrix block) are defined. Regards to K' (hydraulic conductivity of the matrix block), it does not contribute to the flow but controls the flux in the block to the fissure. In order to complete the description of the aquifer system, we should introduce a supplementary parameter, b′ (extension of the block to the direction of the flux). These parameters are defined with supposing that each "point" is occupied simultaneously by the two porosities which extend to the totality of the transverse extension of the aquifer. That may be understood by the representative elementary volume or REV (Bear, 1972, pp.19−20) such that it covers a sufficient quantity of each of the porosities. Hence, the REV should be great enough compared to the scale of fracturation.

This model is a generalized model of Boulton and Streltsova(1977).

The differential equation of the drawdown $s_2(r,t)$ in the unit of matrix blocks is as follows (Boulton et Streltsova, 1977) :

$$\frac{\partial^2 s_2}{\partial z^2}=\frac{S_s'}{K'}\frac{\partial s_2}{\partial t} \quad \cdots\cdots(1)$$

where

K' : hydraulic conductivity of the matrix block (LT^{-1})

S_s' : specific storage of the matrix block (L^{-1})

s_2 : drawdown in the matrix block (L)

z : distance from a point in the block to the fracture to the direction of flux (L)

t : time since pumping started (T).

The equation of drawdown $s_1(r,t)$ in the unit of fissures can be expressed :

$$\frac{K_f}{r^{n-1}}\frac{\partial}{\partial r}\left(r^{n-1}\frac{\partial s_1}{\partial r}\right)=S_{sf}\frac{\partial s_1}{\partial t}-v \quad \cdots\cdots(2)$$

where

K_f : hydraulic conductivity of the fracture (LT^{-1})

S_{sf} : specific storage of the fracture (L^{-1})

s_1 : drawdown in the fracture (L)

r : radial distance from the production well, along the flow line (L)

v : rate of flux from the matrix block to the fissure (T^{-1}) , $v=\frac{K'}{b'}\left(\frac{\partial s_2}{\partial z}\right)_{z=0}$

n : fractal dimension of flow.

We assume that the fractal system obeys Darcy's law. Consequently, the change of storage in the well can be given by :

$$W_s\frac{\partial s_w}{\partial t}=Q+K_f b^{3-n}\alpha_n r_w^{n-1}\left(\frac{\partial s_1}{\partial r}\right)_{r=r_w} \quad \cdots(3)$$

where

Q : discharge rate (L^3T^{-1})

s_w : drawdown at the production well (L)

s_f : skin factor (dimensionless)

W_s : storage capacity of the production well (L^2)

r_w : radius of the production well (L)

b : transverse extension of the fractures to the flow path (L)

$\alpha_n=2\pi^{n/2}/\Gamma(n/2)$

$\Gamma(n/2)$: gamma function.

The drawdown in the production well will be different from the drawdown at $r=r_w$ if there exists a skin loss :

$$s_w(t)=s_1(r_w,t)-s_f r_w\left(\frac{\partial s_1}{\partial r}\right)_{r=r_w} \quad \cdots\cdots(4)$$

The initial conditions and the boundary conditions are :

$s_w(r,0)=s_1(r,0)=s_2(r,0)=0$ for all the distance r

$s_1(\infty,t)=s_2(\infty,t)=0$ for all the time t

Let us define the following dimensionless parameters :

$$t_D=\frac{4K_f t}{(S_{sf}+S_s')}r_w^2 \quad \cdots\cdots(5)$$

$$r_D=r/r_w \quad \cdots\cdots(6)$$

$$z_D=z/b' \quad \cdots\cdots(7)$$

$$\lambda=\frac{K' r_w^2}{K_f b'^2} \quad \cdots\cdots(8)$$

$$\omega=\frac{S_{sf}}{S_{sf}+S_s'} \quad \cdots\cdots(9)$$

$$s_{1D}=\frac{4\pi^{n/2}K_f b^{3-n}}{Q r_w^{2-n}}s_1 \quad \cdots\cdots(10)$$

$$s_{2D}=\frac{4\pi^{n/2}K_f b^{3-n}}{Q r_w^{2-n}}s_2 \quad \cdots\cdots(11)$$

$$W_{sD}=\frac{W_s}{\pi^{n/2}b^{3-n}r_w^n(S_{sf}+S_s')} \quad \cdots\cdots(12)$$

Using the dimensionless parameters, we can write equations (1), (2), (3) and (4) in dimensionless forms :

$$\frac{\partial^2 s_{2D}}{\partial z_D^2}=\frac{4(1-\omega)}{\lambda}\frac{\partial s_{2D}}{\partial t_D} \quad \cdots\cdots(13)$$

$$\frac{1}{r_D^{n-1}}\frac{\partial}{\partial r_D}\left(r_D^{n-1}\frac{\partial s_{1D}}{\partial r_D}\right)=4\omega\frac{\partial s_{1D}}{\partial t_D} -\lambda\left(\frac{\partial s_{2D}}{\partial z_D}\right)_{z_D=0} \quad \cdots\cdots(14)$$

$$W_{sD}\frac{\partial s_{wD}}{\partial t_D}=1+\frac{1}{2\Gamma(n/2)}\left(\frac{\partial s_{1D}}{\partial r_D}\right)_{r_D=1} \cdots(15)$$

$$s_{wD}(t_D)=s_{1D}(1,t_D)-s_f\left(\frac{\partial s_{1D}}{\partial r_D}\right)_{r_D=1} \cdots\cdots(16)$$

Transforming the equations (13)－(16) in the space of Laplace gives

$$\frac{d^2\bar{s}_{2D}}{dz_D^2}=\frac{4p(1-\omega)}{\lambda} \quad \cdots\cdots(17)$$

$$\frac{d^2\bar{s}_{1D}}{dr_D^2}+\frac{n-1}{r_D}\frac{d\bar{s}_{1D}}{dr_D}+\lambda\left(\frac{d\bar{s}_{2D}}{dz_D}\right)_{z_D=0} =4p\omega\bar{s}_{1D} \quad \cdots\cdots(18)$$

$$pW_{sD}\bar{s}_{wD}=\frac{1}{p}+\frac{1}{2\Gamma(n/2)}\left(\frac{d\bar{s}_{1D}}{dr_D}\right)_{r_D=1} \cdots(19)$$

$$\bar{s}_{wD}(p)=\bar{s}_{1D}(1,p)-s_f\left(\frac{d\bar{s}_{1D}}{dr_D}\right)_{r_D=1} \cdots\cdots(20)$$

The general solution of the equation (17) in the space of Laplace is expressed :

$$\bar{s}_{2D}(z_D,p)=A\cosh(\eta z_D)+B\sinh(\eta z_D) \quad \cdots\cdots(21)$$

where

$$\eta^2=\frac{4p(1-\omega)}{\lambda} \quad \cdots\cdots(22)$$

When $z_D=1$,

$$\frac{d\bar{s}_{2D}}{dz_D}=0 \quad \cdots\cdots(23)$$

Consequently,

$$B=-A\tanh(\eta) \quad \cdots\cdots(24)$$

If we consider the fracture skin (Moench, 1984).

$$s_{2D}=s_{1D}+b'S_F\left(\frac{\partial s_{2D}}{\partial z_D}\right)_{z_D=0} \cdots\cdots(25)$$

where $S_F=K'b_s/K_s b'$, dimensionless fracture skin

K_s=hydraulic conductivity of the fracture skin(LT^{-1})

b_s=thickness of the fracture skin(L).

If there is no fracture skin,

$$s_{2D}=s_{1D} \quad \cdots\cdots(26)$$

The fracture skin impedes the flux of the matrix block to the fracture owing to a lower hydraulic conductivity of the fracture skin than that of the matrix block (Fig. 1). The fracture skin may be derived from a low permeability zone which is made by the deposition of minerals or by chemical alteration. The Laplace transform of the equation(25) is :

$$\bar{s}_{2D}=\bar{s}_{1D}+S_F\left(\frac{d\bar{s}_{2D}}{dz_D}\right)_{z_d=0} \quad \cdots\cdots(27)$$

Since

$$\left(\frac{d\bar{s}_{2D}}{dz_D}\right)_{z_D=0}=-A\ \eta\tanh(\eta) \quad \cdots\cdots(28)$$

and

$$\bar{s}_{2D}=A \quad \cdots\cdots(29)$$

the coefficient A is determined :

$$A=\frac{\bar{s}_{1D}}{1+S_F\eta\tanh(\eta)} \quad \cdots\cdots(30)$$

Hence, from the equations (21), (24) and (30),

$$\bar{s}_{2D}=\frac{\bar{s}_{1D}}{1+S_F\eta\tanh(\eta)}[\cosh(\eta z_D)-\tanh(\eta)\sinh(\eta z_D)] \quad \cdots\cdots(31)$$

When we take the average of drawdowns in the matrix block by the integration on z_D from the height 0 to b′, the equation (31) can be rearranged :

$$\bar{s}_{2D}=\frac{\bar{s}_{1D}\tanh(\eta)}{\eta[1+S_F\ \eta\tanh(\eta)]} \quad \cdots\cdots(32)$$

If there is no fracture skin,

$$\bar{s}_{2D}=\bar{s}_{1D}[\cosh(\eta z_D)-\tanh(\eta)\sinh(\eta z_D)] \quad \cdots\cdots(33)$$

The general solutions of dimensionless drawdown at the production well and in the fractures are (Hamm, 1994) :

$$\bar{s}_{wD}=\frac{1}{p\left[pW_{sD}+\frac{1}{2\Gamma(n/2)}\frac{1}{K^v_{v-1}(\sigma)+s_f}\right]} \quad \cdots\cdots(34)$$

$$\bar{s}_{1D}=\frac{1}{p}\frac{1}{\left[pW_{sD}+\frac{1}{2\Gamma(n/2)}\frac{1}{K^v_{v-1}(\sigma)+s_f}\right]}\frac{r_D^vK_v(\sigma r_D)}{K_v(\sigma)+s_f\sigma K_{v-1}(\sigma)} \quad \cdots\cdots(35)$$

where

$$\sigma^2=4p\omega+\frac{\lambda\eta\tanh(\eta)}{1+S_F\eta\tanh(\eta)} \quad \cdots\cdots(36)$$

$$K^v_{v-1}(z)=\frac{K_v(z)}{zK_{v-1}(z)} \quad \cdots\cdots(37)$$

and $v=1-n/2$ $\cdots\cdots(38)$

The Eqs. (32), (34) and (35) can be inverted into the real plane, using Stehfest algorithm (1970). $K_v(z)$ is calculated by Amos package (1986). In Eq. (35), setting wellbore storage to zero and then letting the well radius tend to zero, we obtain :

$$\bar{s}_{1D}=\frac{2^{1+v}}{p}\frac{r_D^vK_v(\sigma r_D)}{\sigma^v} \quad \cdots\cdots(39)$$

THEORETICAL CURVES

Fig. 2 demonstrates some selected theoretical curves of the nonstationary dual-porosity fractal (NDPF) model with different values of r_w/b' for the production well and for the dimensions 1, 1.5, 2 and 2.5. One can distinguish three parts on the

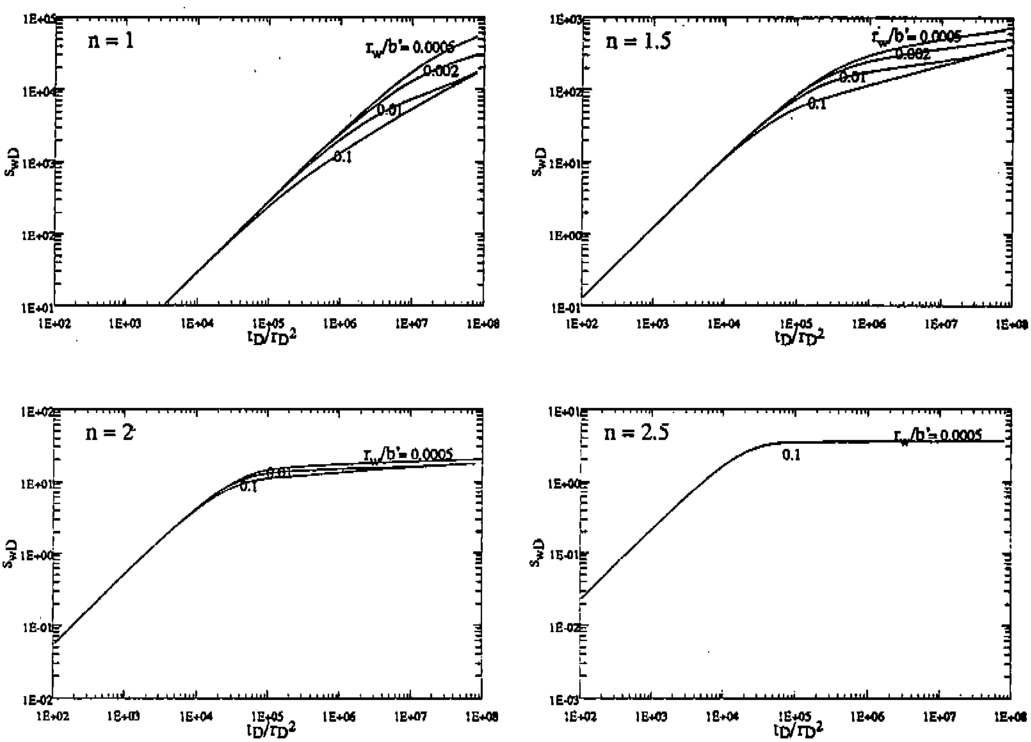

Fig. 2 Selected theoretical curves of the NDPF model with different values of r_w/b' for the production well and for the fractal dimensions 1, 1.5, 2 and 2.5. W_s=0.03m² is used.

curves. The first part represents wellbore storage effect followed by flow in the fracture. The portion concerning welbore storage effect shows a straight line with a slope of 1. The second part reflects the progressive contribution of water from the matrix block to the fissure. Finally, the third part shows the response of the total system of both the fissure and the matrix block.

Fig. 3 illustrates selected theoretical curves of the NDPF model with different values of r/b′ for the observation well in the fissure, and for the dimensions 1, 1.5, 2 and 2.5. The curves are composed of three parts. The first part reflects the contribution only from the fissure. The second part represents the progressive contribution of water from the matrix block. The third part represents the response of the total system of both the fissure and the matrix block, and the curve becomes that of Barker's model. The duration of the second part is dependant on ω. The level of drawdown depends on λ. It is noticeable that for the same value of r/b′, when the dimension of flow is larger, dimensionless drawdown is higher in the first part, and it is lower in the last part. For the same dimension, when the value of r/b′ is larger,

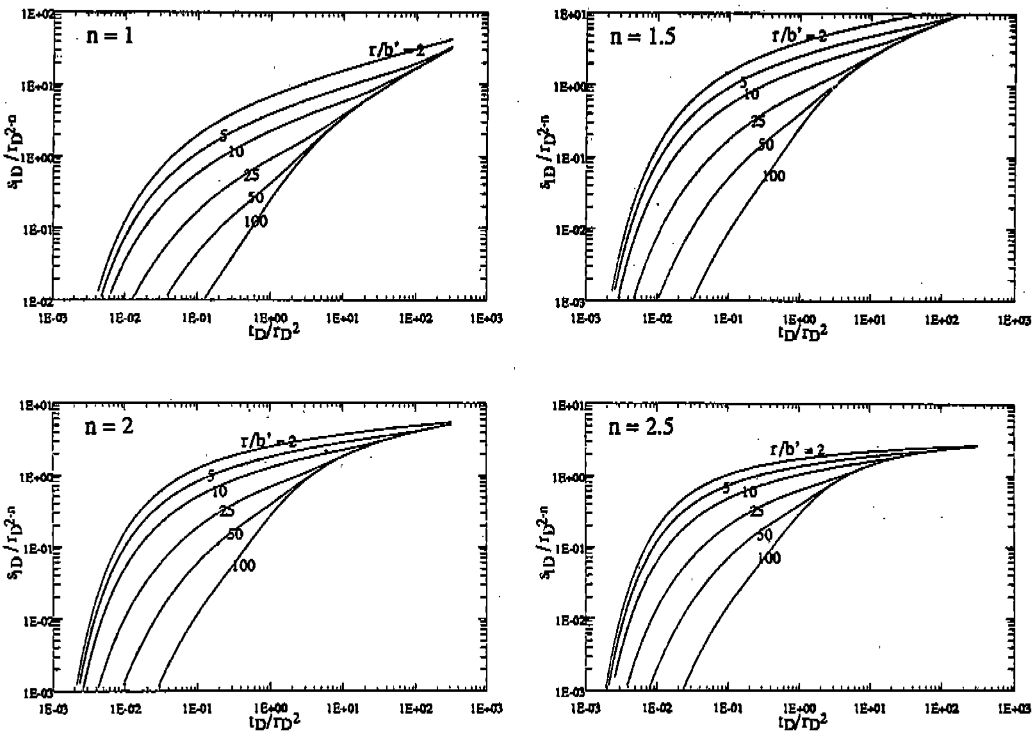

Fig. 3 Selected theoretical curves of the NDPF model with different values of r/b' for the observation well in the fracture, and for the fractal dimensions 1, 1.5, 2 and 2.5.

the drawdown is smaller. Furthermore, for different dimensions, when the value of r/b' is small, the point of intersection is met rapidly.

Fig. 4 shows the curves of the matrix block. The bigger the value of r/b', the more the curve approaches that of Barker's model. On the contrary, when r/b' is small, the curve has a sraight line in the first part and joins the curve of fracture. For the same value of r/b', the slope of the curve is gentle with an increase in dimension. Moreover, for the same value of r/b', the greater the dimension, the greater the drawdown in the early part, and the smaller it is in the last part. For different dimensions, the smaller the value of r/b', the earlier the point of intersection. The difference of dimensionless drawdown between different dimensions is becoming great with a decrease in the value of r/b'. Inversely to the case of the fissure, for the same dimension, when the value of r/b' is great, the drawdown is also great.

Fig. 5 displays selected theoretical curves of the NDPF model with different values of the fracture skin (S_F) for the abstraction well, and for the dimensions 1, 1.5, 2 and 2.5. We used $W_s=10^4m^2$ and $r_w/b'=0.01$. As the case of the production well of the non-

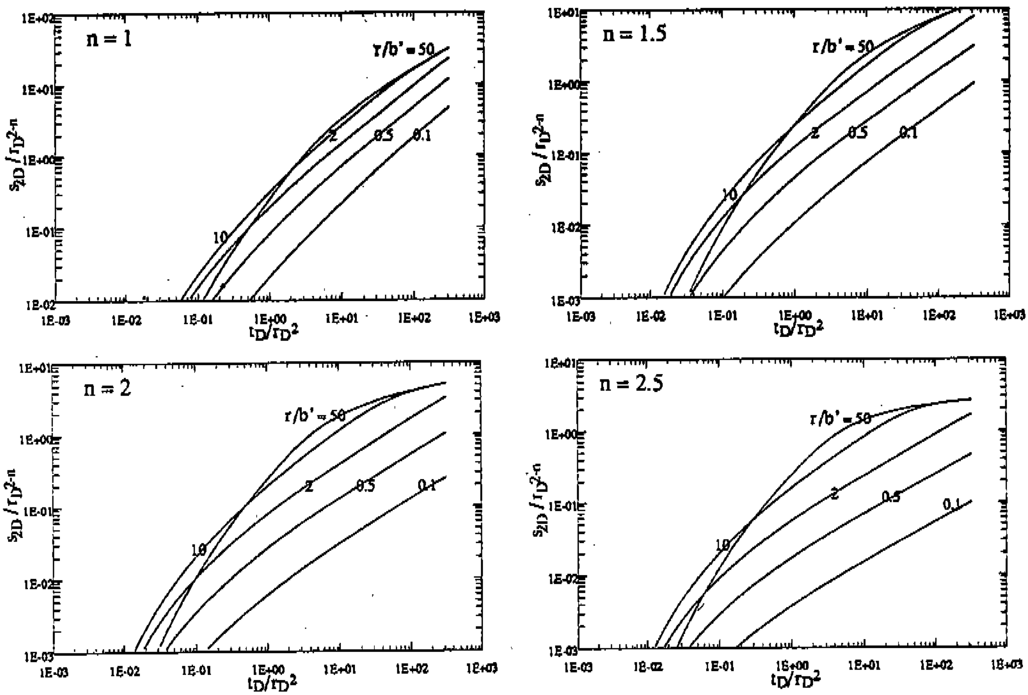

Fig. 4 Selected theoretical curves of the NDPF model with different values of r/b' for the observation well in the matrix block, and for the fractal dimensions 1, 1.5, 2 and 2.5.

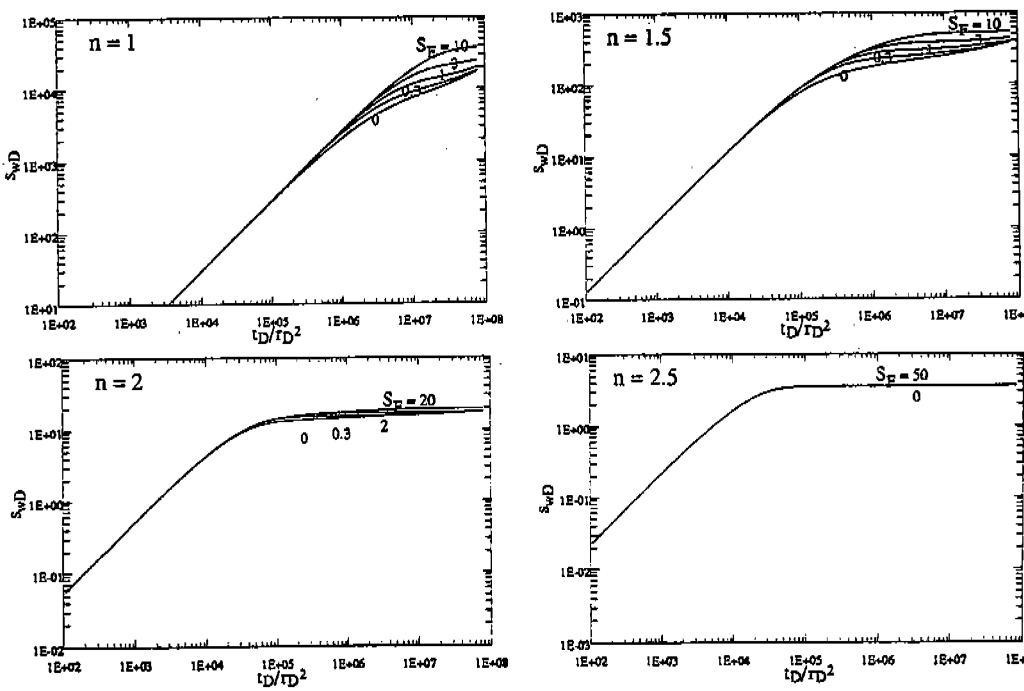

Fig. 5 Selected theoretical curves of the NDPF model with different values of the fracture skin (S_F) for the production well and for the fractal dimensions 1, 1.5, 2 and 2.5. W_s=0.03m^2 is used.

steady state dual-porosity fractal model, they show three parts on the curves : the first part of the wellbore storage followed by the flow in the fissure, the second part of the flow in the fissure plus the contribution from the matrix block and the third part of the flow in the uniform system of the fissure and the block. When S_F increases, the slope of the second part is gentle.

Fig. 6 shows selected theoretical curves of the NDPF model with different values of the fracture skin (S_F) for the observation well in the fissure, and for the dimensions 1, 1.5, 2 and 2.5. $r/b' = 5$ is used. The curves are composed of three parts. The early part of the curves represents the flux from fractures. The intermediary part represents water supply from the matrix block progressively so that the rate of drawdown diminishes. The last part represents the contribution form both the fracture and the matrix block. When S_F is large, drawdown is also large.

Fig. 7 shows selected theoretical curves of the NDPF model with different values of the fracture skin (S_F) for the observation well in the matrix block, and for the dimensions 1, 1.5, 2 and 2.5. The

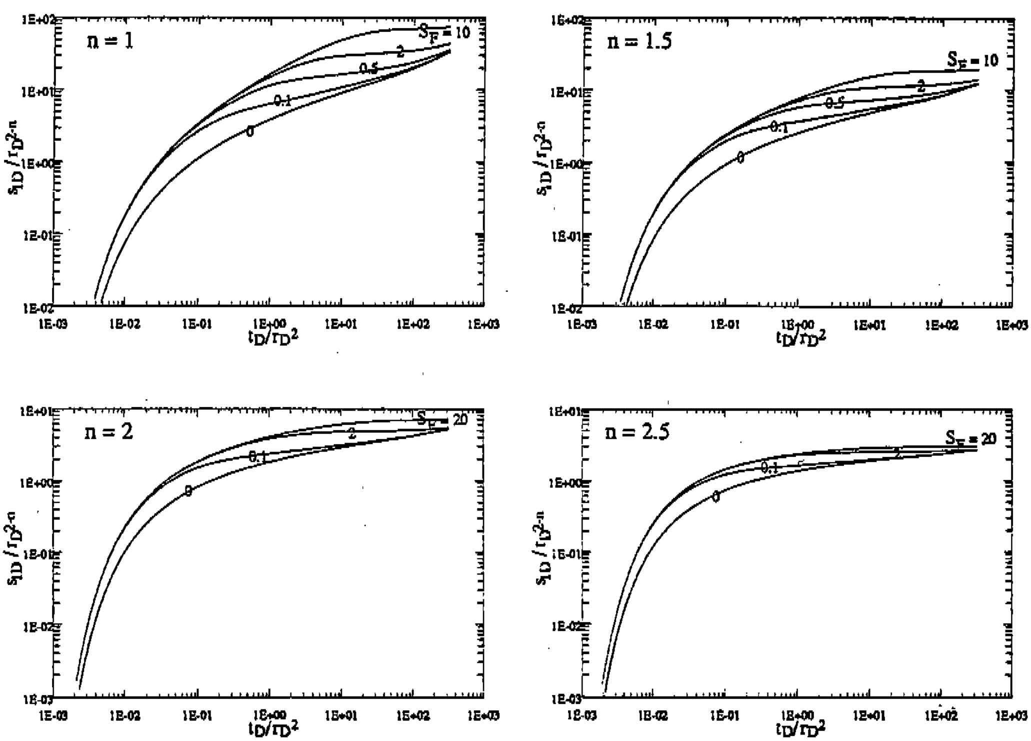

Fig. 6 Selected theoretical curves of the NDPF model with different values of the fracture skin (S_F) for the observation well in the fracture, and for the fractal dimensions 1, 1.5, 2 and 2.5.

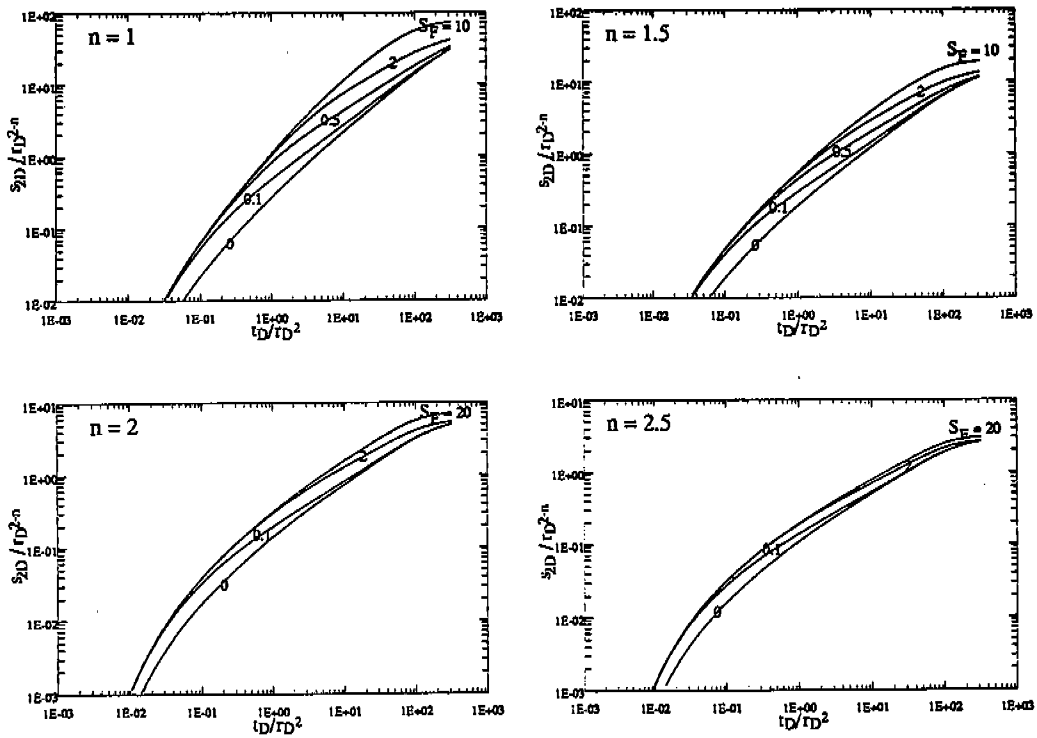

Fig. 7 Selected theoretical curves of the NDPF model with different values of the fracture skin (S_F) for the observation well in the matrix block, and for the fractal dimensions 1, 1.5, 2 and 2.5.

dimensionless drawdown in the matrix block (s_{2D}/r_D^{2-n}) is the average value over b′ of the matrix block. r/b′ = 5 is used. The response of dimensionless drawdown of the matrix block is later than that of the fissure, and the rate of drawdown is faster than that of the fissure.

APPLICATION

The NDPF model was applied to typical experimental data of the Pocheon site. Two wells (No.1 and No.2) have been utilized for pump test analysis. No.1 is the pumped well of the depth of 600m, and No.2 is the observation well of the depth unknown (Lim et al., 1990). The distance between No.1 and No.2 is 240m.

The geology at the well No.1 is composed of biotite granites. According to temperature and gamma-ray loggings, the most important aquifers are situated in the interval between 405m and 415m, and the interval between 475m and 500m.

The pump test has been executed with a discharge rate of $7.3\times10^{-3}m^3s^{-1}$ for 24hours(Lim et al., 1990). The drawdown was observed at the production well and the

Table 1. Calculated hydraulic parameters.

Site	$K_f b^{3-n}$ ($m^{4-n}sec^{-1}$)	K_f/S_{sf} (m^2sec^{-1})	$K'b'^{3-n}$ ($m^{4-n}sec^{-1}$)	K'/S_s' (m^2sec^{-1})	n	S_F	s_f	W_s (m^2)	PI (m^2sec^{-1})
Pocheon	3.25×10^{-3}	28	3.7×10^{-5}	2.0×10^{-4}	1.45	0	66	0.018	9.1×10^{-5}

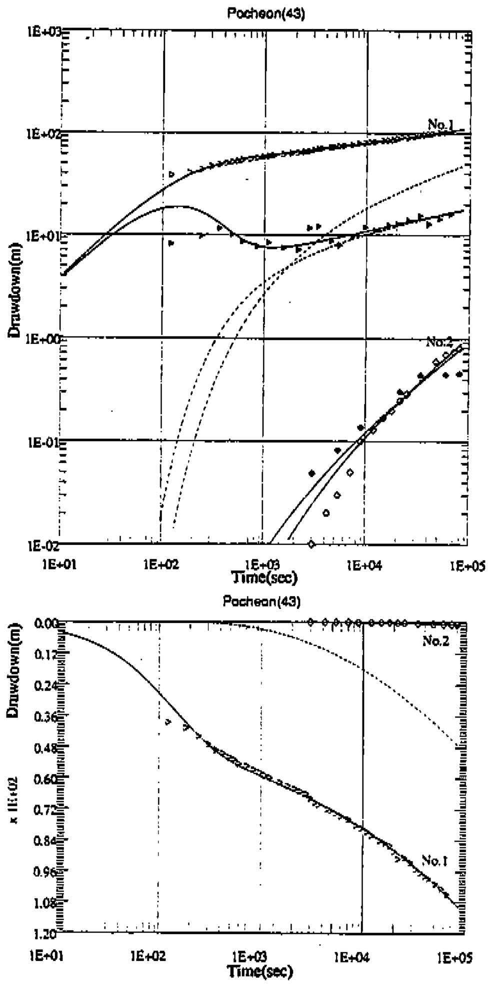

Fig. 8 Theoretical curves and observed curves at the pumping well (No.1) and the observation well (No.2), Pocheon site. Void triangle and black triangle represent observed drawdowns and derivatives of the observed drawdowns, respectively. Corresponding curves represent theoretical drawdowns and derivatives of the theoretical drawdowns.

observation well. For the pump test analysis, the value of the specific storage in the fractures is fixed as $5\times10^{-6}m^{-1}$ and that in the matrix block as 5×10^{-5} m^{-1} (Walton, 1970). The observed curve completely deviates from the Theis curve. Its derivative curve shows a typical form of the NDPF model. As a result of the analysis, the theoretical curves and the observed data show a good accordance at the pumping well and the observation well simultaneously (Fig. 8). One remarkable thing is that the drawdown curve of the observation well represents that of matrix block, not fissure. From the calulation, the flow dimension is determined 1.45 and the specific capacity (PI) $9.1\times10^{-5}m^2\cdot sec^{-1}$ (Table 1). One explanation of the hydrodynamic situation is that similar to bilinear flow with an important fracture (Cinco-Ley and Samaniego, 1981).

CONCLUSION

The NDPF model can reasonably describe the hydraulic property of fractured aquifers having double porosity while Boulton-Streltsova model and Moench model are not sufficient to do it because fractured aquifers often have fractal geometries. Hence, the new model can be used as a more versatile tool to analyze pumping test data from fractal and fractured media. The model can take into account the wellbore storage and the well loss effects on the production well. It can also be easily applied to the multi-well and multi-rate pumping system composed of several production and observation wells.

An application of the model to field data in Pocheon site gives 1.45 of the flow dimension.

REFERENCES

Allègre, C. J., le Mouël, J. L. and Provost, A., 1982, Scaling rules in rock fractures and possible implications for earthquake prediction, Nature, v.297, pp.47−49.

Amos, D.E., 1986, A portable package for Bessel functions of complex argument and nonnegative order, ACM Trans. Math. Software, v.12, n.3, pp.265-273.

Barenblatt, G.E., Zheltov, I.P. and Kochina, I.N., 1960, Basic concepts in the theory of seepage of homogeneous liquids in fissured rocks, Jour. Appl. Math. Mech. Engl. Transl., v.24, n.5, pp.1286−1303.

Barker, J.A., 1988, A generalized radial flow model for hydraulic tests in fractured rock, Water Resour. Res., v. 24, n.10, pp.1796−1804.

Bear, J., 1972, Dynamics of fluids in porous media, American Elsevier Publishing Company, Inc., New York, p.764.

Boulton, N.S. and Streltsova, T.D., 1977, Unsteady flow to a pumped well in a fissured water-bearing formation, Jour. Hydr., v.35, pp.257-269.

Chang, J. and Yortsos, Y.C., 1988, Pressure transient analysis of fractal reservoirs, SPE 18170, pp.1-14.

Cinco-Ley, H. and Samaniego-V., F., 1981, Transient pressure analysis for fractured wells, J. Pet. Tech., v.33(Sept.), pp.1749-1766.

Hamm, S. Y., 1994, Nouveaux models fractals d'écoulement dans les milieux fissurés : application aux données de pompages en Corée du Sud, Thèse Doctorat ès Sciences, Université de Montpellier II, p.243.

Hamm, S. Y. and Bidaux, P., 1994a, Ecoulements transitoires en géométrie fractale avec drainance : théorie et application, C. R. Acad. Sci. Paris, 318, série II, n.2, pp.227−233.

Hamm, S. Y. and Bidaux, P., 1994b, Stationary dual-porosity fractal model of groundwater flow in fractured aquifers, The Jour. Eng. Geol. v.4, n.2, pp.127-138.

Kazemi, H., 1969, Pressure transient analysis of naturally fractured reservoirs with uniform fracture distributions, Trans. Soc. Pet. Eng., AIME, v. 246, pp.451-462.

Lim, J. U. et al., 1990, Investigation report of geothermal potential, Shinbook-myeon, Pocheon area, Korea Institute of Energy and Resources.

Moench, A. F., 1984, Double-porosity models for a fissured groundwater reservoir with fracture skin, Water Resour. Res., v.20, n.7, pp.831-846.

Stehfest, H., 1970, Numerical inversion of Laplace transforms, Commun. ACM, v. 13, n.1, pp.47-49.

Streltsova, T.D., 1976, Hydrodynamics of ground water flow in fractured formation, Water Resour. Res., v.12, n.3, pp.405-414.

Thomas, A., 1987, Structure fractale de l'architecture des champs de fractures en milieu rocheux, C. R. Acad. Sci. Paris, 304, sêrie II, pp.181－186.

Velde, B., Dubois, J., Moore, D. and Touchard, J., 1991, Fractal patterns of fractures in granites, Earth and Planetary Science Letters, v.104, pp.25-35.

Warren, J. E. and Root, P. J., 1963, The behavior of naturally fractured reservoirs, SPEJ, v.3, n.2, pp.245-255.

Walton, W.C., 1970. Groundwater Resource Evaluation, McGrwa-Hill, Tokyo, p.664.

함 세 영 :
한국자원연구소
305-350
대전시 유성구 가정동 30번지
TEL : (042)868-3085
FAX : (042)861-9720

Bidaux, Pasal :
Laboratoire d'Hydrogêologie, ERS 82 du CNRS
Univercitê de Montpellier II
place Eugêne Bataillon, 34095 Montpellier Cedex 5, France